*Article*

# Measurements of Bicarbonate in Water Containing Ocean-Level Sulfate Using a Simple Multi-Pass Optical Raman System

**Chetan Shende, Stuart Farquharson \*, Duncan Farquharson and Carl Brouillette**

Real-Time Analyzers, Inc., Middletown, CT 06457, USA; chetan@rta.biz (C.S.);
dfarquharson@hamdenhall.org (D.F.); carl@rta.biz (C.B.)
**\*** Correspondence: stu@rta.biz; Tel.: +86-0-635-9800

**Abstract:** The concentration of dissolved inorganic carbon in the oceans at depths of a few meters to thousands of meters is a critical parameter for understanding global warming. The concentration is both pH dependent and depth dependent. Current analysis that employs pH meters must account for several other parameters, such as salinity, temperature, pressure, and the dissolved carbon's form, carbon dioxide, bicarbonate, or carbonate. Recently, Raman spectroscopy has been used to measure these forms directly in water at ~1000 ppm, which is unfortunately insufficient for typical ocean concentrations, such as ~115 ppm bicarbonate near the surface. Here, we employed a simple multi-pass optical system, a flat mirror to reflect the laser back through the sample, and a concave mirror opposite the entrance slit that effectively doubled the laser power and the collected Raman photons, respectively. This multi-pass optical Raman system with a 1.5 W, 532 nm laser was used to measure 30 ppm bicarbonate in water that contained 2650 ppm sulfate to simulate ocean water, a bicarbonate concentration well below that near the ocean surface. Furthermore, spectral analysis employed the bicarbonate C=O symmetric stretch at 1360 $cm^{-1}$ instead of the C–OH stretch at 1015 $cm^{-1}$ to avoid the intense, overlapping sulfate $SO_4$ symmetric stretch at 985 $cm^{-1}$. The calculated standard deviation of ~5 ppm for the described approach suggests that accurate measurement of bicarbonate in situ is possible, which has been, heretofore, either calculated based on pH or measured in a lab.

**Keywords:** ocean carbon dioxide; bicarbonate; Raman spectroscopy

## 1. Introduction

The measurement of dissolved inorganic carbon in the ocean has taken on considerable importance in view of the increasing emissions of $CO_2$ into the atmosphere which, when sequestered, acidifies the oceans [1,2], negatively affecting coral reefs [3], crustaceans [4], and many other carbonate-containing aquatic life forms. In light of these deleterious effects, a controversial proposal [5] suggests that pumping $CO_2$ into the oceans below 3000 m [6], where it is denser than water, could remove substantial amounts of $CO_2$ from the atmosphere, alleviating global warming [7]. Currently, pH meters are used to estimate the amount of $CO_2$ in the water based on the equilibrium of Equation (1) [8], a classic Bjerrum pH dependent reaction.

$$CO_2 + H_2O \rightleftharpoons H_2CO_3 \rightleftharpoons H^+ + HCO_3^- \rightleftharpoons 2H+ + CO_3^{2-} \tag{1}$$
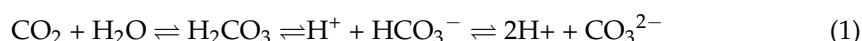
Unfortunately, pH alone is not sufficient as it only measures hydrogen ions, and has underestimated the $CO_2$ concentration in non-equilibrium cases, such as at ocean depths below 3000 m [9]. Several researchers have demonstrated the ability of Raman spectroscopy to perform these measurements. Scientists at the Canadian Department of the Environment, Inland Waters Branch, demonstrated that $CO_2$, bicarbonate ($HCO_3^-$) and carbonate ($CO_3^{2-}$) all produce unique vibrational modes that could be used for quantitation [10]. The 2014 concentration for these species in the ocean at a pH of 8 are $CO_2$ at 0.9 ppm, $HCO_3^-$ at 114 ppm and $CO_3^{2-}$ at 9.5 ppm (mg/L) [11]. The researchers

at Monterey Bay Aquarium Research Institute developed a sophisticated two chamber sample system to mix liquid $CO_2$ and seawater at a depth of 500 m and measured both the pH and Raman spectra [12,13]. The spectrometer, using a 50 mW, 532 nm laser and a $-100\ ^\circ C$ thermal-electrically cooled (TEC) detector, (36 cm diameter, 80 cm long, 180 kg, not including the probe head) was able to measure 1080 ppm $CO_2$ in 2.5 min, based on the $1380\ cm^{-1}$ peak area, with an estimated limit of detection of 600 ppm. This system may have value in monitoring $CO_2$ near the 3000 m condensation depth, especially if pumping it into the ocean is implemented. The team at the Ocean University of China developed a multi-pass optical sample system that provided a 7.8 signal amplification factor for a spectrometer using a 300 mW, 532 nm laser and a $-80\ ^\circ C$ TEC detector. The system was used to measure ~1600 ppm $CO_2$ ppm gas phase extracted from a liquid water sample in 3 min [14]. Based on these previous systems we developed a Raman system that used a high powered 1.5 W, 532 nm laser and a simple multiplicative optical system and measured $CO_2$, $HCO_3^-$, and $CO_3^{2-}$ in 20 min at tens of ppm concentrations in water [15,16]. Here, we present measurements of $HCO_3^-$ in water containing 2650 ppm sulfate to simulate the spectral challenge of performing measurements in the ocean. The calculated error of $\pm 3$ ppm in the measurement is close to the highest yearly flux of 2 ppm for the ocean [17].

## 2. Materials and Methods

Materials. Potassium bicarbonate ($KHCO_3$), sodium sulfate ($NaSO_4$), and HPLC grade water were purchased from Sigma Aldrich. A stock solution of 2650 ppm sulfate in HPLC grade water was prepared and used to prepare two bicarbonate dilution series, Series 1: 1000, 3000, 1000, 300, 150, 100 and 30 ppm; Series 2: 1000, 500, 250, 200, 125, 100 and 50 ppm. The samples were added to 3.5 mL quartz cuvettes, each with four optical sides, an optical pathlength of 10.0 mm and $1.25 \pm 0.10$ mm wall thickness, and sealed with Teflon caps (ThorLabs, Newton, NJ, USA) and parafilm (VWR, Radner, PA, USA).

Methods. The Raman spectrometer employed a 1.5 W, 532 nm laser (model Cobolt Samba 1500 532 nm, Hubner Photonics, San Jose, CA, USA) and a $-15\ ^\circ C$ cooled 2048 pixel Si detector (model 532-C-SR-L-25, Wasatch Photonics, Morrisville, NC, USA). Spectra were recorded from ~200 $cm^{-1}$ to 3200 $cm^{-1}$ with ~20 $cm^{-1}$ resolution (peak width at half height) and peak positions are reported to the nearest 5 $cm^{-1}$. Initially, Raman spectra were collected using 180° backscattering geometry. However, the laser induced a substantial $SiO_2$ background from the pre-sample optics, particularly the long wavelength pass filter that was used to reflect the laser into the sample and transmit the generated Raman photons into the spectrograph in the 180° backscatter arrangement. Consequently, this component was removed and a 90° perpendicular collection arrangement was employed (Figure S1). While the $SiO_2$ spectral features were removed, a substantial tilted background remained due to the laser baseline "wings" in spite of the use of two additional long wavelength pass filters with an optical density of 6 (Semrock, Rochester, NY, USA) inside the spectrograph. In addition, a flat mirror was used to reflect the laser 180° back through the sample to generate more Raman photons, while a 9 mm diameter f/0.5 concave mirror (Edmund Optics, Barrington, NJ, USA) was mounted opposite the spectrograph entrance to reflect and focus the Raman photons scattered away from the spectrograph back towards the spectrograph. Both mirrors were front-coated with silver. A simple plastic enclosure was built to confine the potentially blinding laser. Wasatch software (Dash v3.2) was used to set the TEC detector temperature, while Hubner Photonics software (Cobolt Monitor 6.0.6.0) was used to turn the laser on and off, and set the power. RTA collection software (Raman Vista 3.4.17) was used to set the integration time, number of integrations, and collect "dark and light", laser off and on spectra, the former automatically subtracting from the latter. RTA software was also used to treat the saved spectra. See individual figure captions for spectral acquisition times.

## 3. Results and Discussion

The challenges to measuring $CO_2$ and $HCO_3^-$ in ocean waters are first, the low concentration on the order of 100 ppm, and second the interference from other chemicals, specifically sulfate at ~2650 ppm. Particulate matter is also a significant source of interference [18], but it is not addressed in this publication. Recently, we developed a highly sensitive Raman spectrometer that was used to measure $HCO_3^-$ and $CO_3^{2-}$ in water at ~30 and 10 ppm, respectively [15]. Key features were the use of a high powered, 1.5 W, 532 nm laser, and two mirrors to increase the Raman generated and collected photons. The spectra were dominated by the water $H_2O$ bending mode at 1640 cm$^{-1}$ [19] and the sulfate $SO_4$ symmetric stretch at 985 cm$^{-1}$ superimposed on a substantial tilted background due to the laser "wings" (Figure 1a). At higher concentrations the bicarbonate C–OH stretch at 1015 cm$^{-1}$ and the C=O symmetric stretch 1360 cm$^{-1}$ were readily observed, more so than the broad and weak C–OH bend at 1300 cm$^{-1}$ (Figure 1a,b) [20].
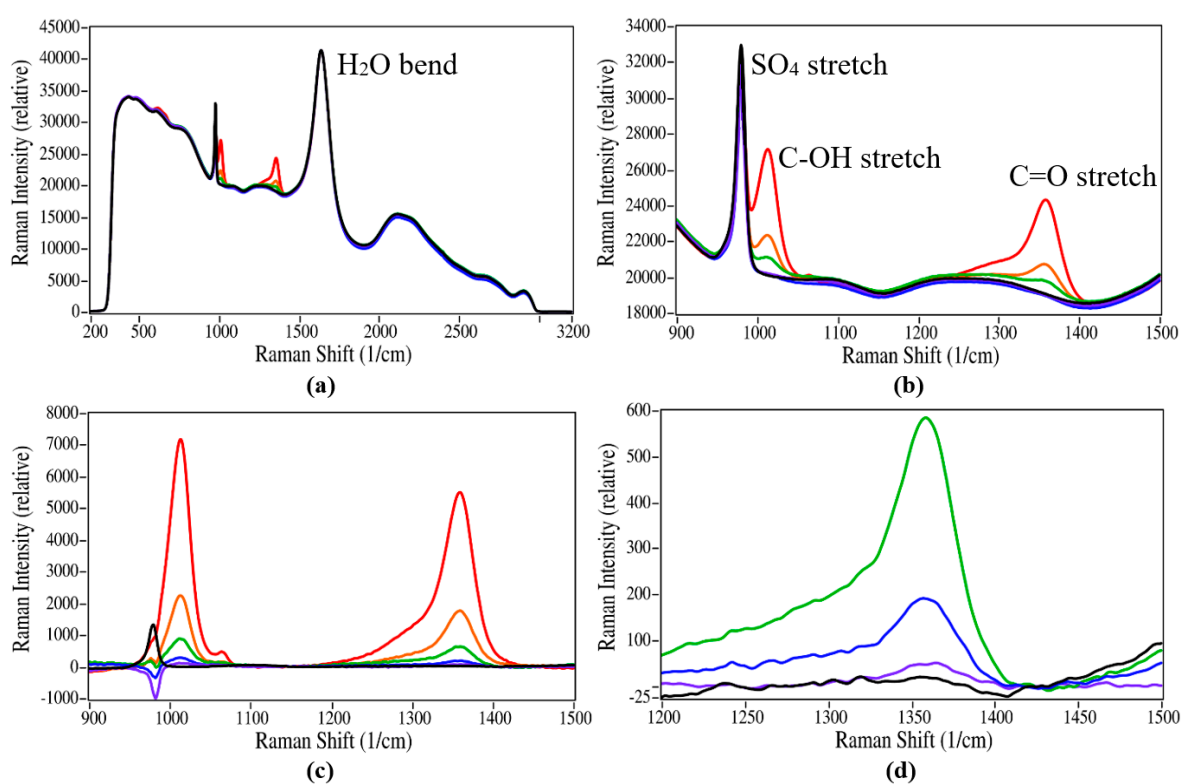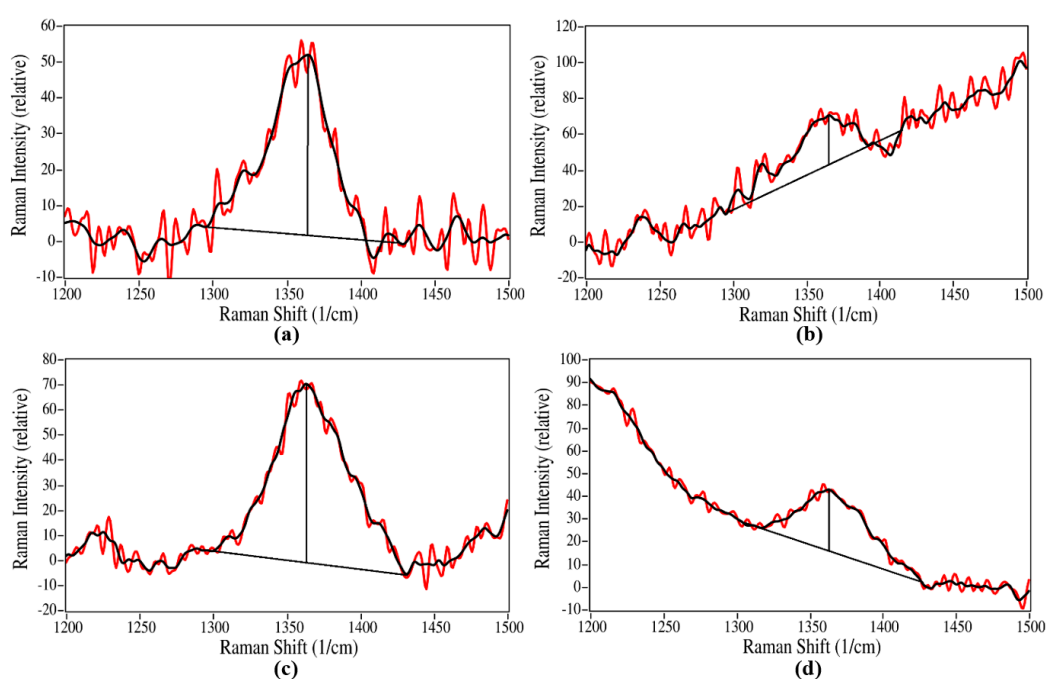


**Figure 1.** Raman spectra of 2650 ppm sulfate in HPLC water plus 10,000 (red), 3000 (orange), 1000 (green), 300 (blue), 100 (purple) and 30 ppm $HCO_3^-$ (black). (**a**) Full spectra, (**b**) expanded view of sulfate and $HCO_3^-$ peaks, (**c**) subtraction of sulfate in water spectrum from all samples by factors of 0.99 to 1.02 with the baseline set to zero at 1415 cm$^{-1}$, and (**d**) 1000 (green), 300 (blue), 100 (purple) and 30 ppm $HCO_3^-$ (black) spectra fit with a 3rd-order 19-point smooth. Conditions: 1 cm quartz cuvette, 90° collection geometry, flat and concave mirrors, 1.5 W at 532 nm, 240 2-sec integration scans averaged (8 min for 10,000, 3000, and 1000 ppm, 16 min for 300, 100 and 30 ppm $HCO_3^-$).

For this study, two concentration series of $HCO_3^-$, Series 1: 10,000 to 30 ppm and Series 2: 1000 to 50 ppm, were prepared in water containing sulfate at 2650 ppm, and measured with the high powered, dual mirror Raman system. The $H_2O$ bending mode was used as an internal intensity standard, to which all spectra were scaled for analysis. The $HCO_3^-$ 1015 cm$^{-1}$ peak is usually preferred to the 1360 cm$^{-1}$ peak for quantitation, because the former is more intense and the latter overlaps the broad 1300 cm$^{-1}$ peak [14,15]. Although the $HCO_3^-$ 1015 cm$^{-1}$ peak is easily discerned at 10,000, 3000, and 1000 ppm, at lower concentrations it becomes obscured by the high background spectrum and interfered by the sulfate peak at 985 cm$^{-1}$, which has a scattering cross section more than six times that

of the $HCO_3^-$ 1015 cm$^{-1}$ peak [21]. Fitting the overlapping sulfate-bicarbonate peaks with weighted amounts of the individual chemical spectra involves user selected parameters, such as spectral region, peak shape and width, as well as baseline corrections. All of which can introduce bias in the analysis, especially at concentrations below 300 ppm $HCO_3^-$. Fortunately, the $HCO_3^-$ 1360 cm$^{-1}$ peak is not interfered by sulfate and it was therefore used to quantify the $HCO_3^-$ concentration for all of the samples. A Raman intensity dependent $HCO_3^-$ concentration curve was obtained by performing the following steps. First, the Raman spectrum of the initial sulfate-water solution was subtracted from the sample spectrum until a flat baseline was obtained, and second the spectral baseline was set to 0 at 1415 cm$^{-1}$ (Figure 1c). The amount subtracted ranged from 0.99 to 1.02 for Series 1. It is worth noting that this subtraction resulted in minor over and under subtraction of the sulfate peak. This is due to slight changes in the tilt of the background, which is attributed to the variability of the quartz cuvette wall thickness that can be as much as 10% [22]. Third, the spectral noise was reduced by fitting the spectra with a 3rd-order, 19-point running smooth [23], and fourth, the peak height was measured at 1360 cm$^{-1}$ (Figure 1d).

While this procedure worked well at 100 ppm, the spectra contained considerable noise, and the baseline tilt became significant for lower concentrations, such as 30 ppm (Figure 2). Concentration Series 2 was prepared to focus on the near surface ocean concentration of 115 ppm with the goal of determining the accuracy and precision. This involved preparing and measuring concentrations closer to this value, and increasing the two co-added 8-min spectral acquisition for Series 1 to eight co-added 8-min spectral acquisition for the Series 2 50, 100, and 125 ppm concentrations to improve the signal-to-noise ratio (S/N). While longer acquisitions improved S/N, the baseline tilt remained for the lowest concentration of 50 ppm (Figure 2d). For these lower concentrations a fifth step was used that connected a linear line from 1300 cm$^{-1}$ to 1425 cm$^{-1}$ to account for baseline tilt and determine the peak height at 1360 cm$^{-1}$ (Figure S3). This step eliminates the need for the third step used to set the baseline to zero. This alternative four step sequence can be incorporated into a program to automate analysis.



**Figure 2.** Raman raw (red) and smoothed (black) spectra of 2650 ppm sulfate in HPLC water plus (**a**) 100 and (**b**) 30 ppm $HCO_3^-$ from Series 1, and (**c**) 125 and (**d**) 50 ppm $HCO_3^-$ from Series 2, illustrating baseline correction and simple peak height determination (see Figures S2 and S3). Conditions: 1.5 W at 532 nm, Series 1: two 240 2-Sec integration scans averaged (16 min), Series 2: eight 240 2-Sec integration scans averaged (64 min).

The 1360 cm$^{-1}$ peak heights for the two concentration series were plotted and fit with a straight line (Figure 3). Exceptional fits were obtained with R$^2$ values of 0.9999 and 0.9992, and y intercepts of +11.7 and −4.2 (detector counts normalized to water). The linear fits were used to calculate the concentration for each sample based on the 1360 cm$^{-1}$ peak height, and the difference between the calculated and the prepared concentrations were used to indicate the accuracy of the measurements (Tables 1 and 2). Not surprisingly, the error was greatest for the Series 1 lowest concentration at 22 ± 8 ppm, a 36% difference from the prepared concentration. The Series 2 data were much better, and suggest reasonable accuracy with an average difference of 8 ppm or 3.7% of the prepared concentration.
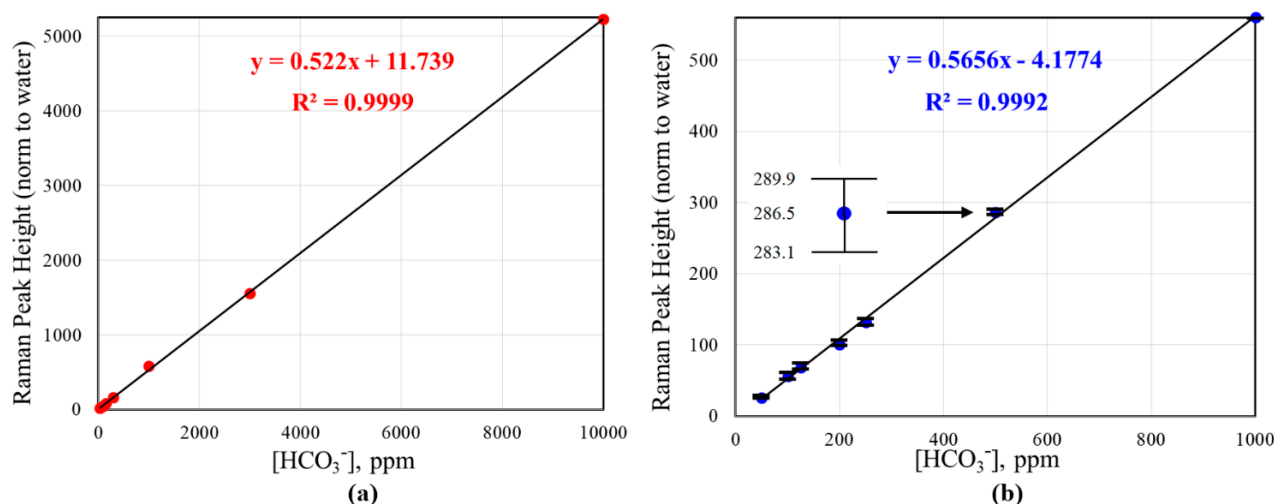


**Figure 3.** Plots of 1360 cm$^{-1}$ Raman HCO$_3{}^-$ peak as a function of concentration in water containing 2650 ppm sulfate, (**a**) Series 1: 0 to 10,000 ppm, and (**b**) Series 2: 0 to 1000 ppm with expanded view of standard deviation for the 500 ppm sample.

**Table 1.** Series 1 prepared HCO$_3{}^-$ concentrations in water containing 2650 ppm sulfate, corrected concentrations based on the linear fit to the data, measured 1360 cm$^{-1}$ peak heights, ppm and percent differences between prepared and corrected calculations, and average values.

| Prepared Concentration (ppm) | 30 | 100 | 150 | 300 | 1000 | 3000 | 10,000 | Average |
|---|---|---|---|---|---|---|---|---|
| Corrected Concentration (ppm) | 22 | 71 | 140 | 299 | 1089 | 2955 | 10,006 | |
| 1360 cm$^{-1}$ Peak Height | 23 | 49 | 85 | 168 | 580 | 1554 | 5235 | |
| Difference (ppm) | 8 | 29 | 10 | 1 | 89 | 45 | 6 | 26.9 |
| % Difference | 36.0% | 41.4% | 6.9% | 0.4% | 8.1% | 1.5% | 0.1% | 13.5% |

**Table 2.** Series 2 prepared HCO$_3{}^-$ concentrations in water containing 2650 ppm sulfate, corrected concentrations based on the linear fit to the data, measured 1360 cm$^{-1}$ peak heights, ppm and percent differences between prepared and corrected calculations, and average values.

| Prepared Concentration (ppm) | 50 | 100 | 125 | 200 | 250 | 500 | 1000 | Average |
|---|---|---|---|---|---|---|---|---|
| Corrected Concentration (ppm) | 54 | 106 | 128 | 186 | 241 | 513 | 997 | |
| 1360 cm$^{-1}$ Peak Height | 26 | 56 | 69 | 101 | 132 | 286 | 560 | |
| Difference (ppm) | 4 | 6 | 3 | 14 | 9 | 13 | 3 | 8.0 |
| % Difference | 6.6% | 5.5% | 2.7% | 7.6% | 3.8% | 2.5% | 0.3% | 3.7% |

The Series 2 individual spectra; eight at 50, 100, and 125 ppm, four at 200, 250, and 500 ppm, and two at 1000 ppm, were used to indicate the precision of the Raman spectrometer measurements (Table 3). For example, the average 1360 cm$^{-1}$ peak height for the 50 ppm prepared sample was 26.4 $\pm$ 1.8, corresponding to 54 $\pm$ 3.7 ppm bicarbonate, a 6.8% standard deviation. In general, the percent standard deviation decreased with increasing concentration, as would be expected. Furthermore, the Series 2 data indicate that Raman spectral measurements are highly reproducible, and therefore, suggest that the inaccuracy of the measurements were likely due to the sample preparation that involved dilution over several orders of magnitude.

**Table 3.** Series 2 prepared $HCO_3^-$ concentrations in water containing 2650 ppm sulfate with repeat 1360 cm$^{-1}$ peak heights, averages, standard deviation and percent standard deviations.

| Prepared Concentration (ppm) | 50 | 100 | 125 | 200 | 250 | 500 | 1000 |
|---|---|---|---|---|---|---|---|
| Measurent 1 (peak height) | 29.1 | 52.2 | 68.9 | 101.5 | 128.9 | 286.7 | 562.9 |
| Measurent 2 (peak height) | 24.8 | 49.4 | 66.9 | 102.2 | 137.9 | 291.3 | 559.0 |
| Measurent 3 (peak height) | 24.6 | 57.9 | 69.3 | 98.4 | 134.1 | 284.0 | |
| Measurent 4 (peak height) | 24.5 | 54.2 | 72.0 | 107.6 | 127.4 | 284.1 | |
| Measurent 5 (peak height) | 28.1 | 58.6 | 66.4 | | | | |
| Measurent 6 (peak height) | 25.5 | 63.2 | 74.3 | | | | |
| Measurent 7 (peak height) | 27.4 | 51.2 | 64.3 | | | | |
| Measurent 8 (peak height) | 27.5 | 59.4 | 76.8 | | | | |
| Average | **26.4** | **55.8** | **69.8** | **102.4** | **132.1** | **286.5** | **561.0** |
| Standard Deviation | 1.8 | 4.7 | 4.2 | 3.8 | 4.8 | 3.4 | 2.8 |
| % Standard Deviation | 6.8% | 8.5% | 6.0% | 3.8% | 3.7% | 1.2% | 0.5% |

## 4. Conclusions

The use of a Raman system employing traditional sample irradiation at 90° to the spectrograph entrance, a high-powered 1.5 W, 532 nm laser, a flat mirror to reflect the laser back though the sample, and a concave mirror to collect Raman scattering opposite the spectrograph entrance, allowed the measurement of $HCO_3^-$ at 30 ppm in water containing 2650 ppm sulfate. Using the bicarbonate C=O symmetric stretch at 1360 cm$^{-1}$, instead of the more intense C-OH stretch at 1015 cm$^{-1}$, avoided interference from the intense, overlapping $SO_4$ stretch at 985 cm$^{-1}$, and allowed a simple series of programmable steps to quantify $HCO_3^-$. The data presented suggest that a Raman system, such as the one described, could measure $HCO_3^-$ accurately, at 125 $\pm$ 4 ppm, directly in the ocean. However, year-to-year changes will require at least a precision of 2 ppm or greater [17].

It would be apropos if Raman spectroscopy, the light scattering phenomenon discovered by Nobel Laureate Sir Chandrasekhar Venkata Raman as he wondered why the oceans appear blue even on cloudy days [24], became the method of choice to monitor the Reaction 1 components in the oceans, which in turn allowed understanding and alleviating global warming and aquatic life mortality.

## References

1. Kleypas, J.A.; Feely, R.A.; Fabry, V.J.; Langdon, C.; Sabine, C.L.; Robbins, L.L. Impacts of Ocean Acidification on Coral Reefs and Other Marine Calcifiers: A Guide for Future Research. In *Report of a Workshop Held*; NOAA: St. Petersburg, FL, USA, 2005.
2. Caldeira, K.; Wickett, M.E. Anthropogenic carbon and ocean pH. *Nature* **2003**, *425*, 365. [CrossRef] [PubMed]
3. Mollica, N.R.; Guo, W.; Cohen, A.L.; Huang, K.-F.; Foster, G.L.; Donald, H.K.; Solow, A.R. Ocean acidification affects coral growth by reducing skeletal density. *Proc. Natl. Acad. Sci. USA* **2018**, *115*, 1754–1759. [CrossRef] [PubMed]
4. Taylor, J.R.A.; Gilleard, J.M.; Allen, M.C.; Deheyn, D.D. Effects of $CO_2$-induced pH reduction on the exoskeleton structure and biophotonic properties of the shrimp *Lysmata californica*. *Nat. Sci. Rep.* **2015**, *6*, 1–12. [CrossRef]
5. Pearce, F. What Is the Carbon Limit? That Depends Who You Ask. Yale Envrironment360. 6 November 2014. Available online: https://e360.yale.edu/features/what_is_the_carbon_limit_that_depends_who_you_ask (accessed on 15 December 2020).
6. Adams, E.E.; Caldeira, K. Ocean Storage of $CO_2$. *Elements* **2008**, *2*, 319–324. [CrossRef]
7. Friederici, P. Ocean Carbon Sequestration: The World's Best Bad Idea. In *Pacific Standard*; The Social Justice Foundation: Santa Barbara, CA, USA, 2017.
8. Witze, A. Southern Ocean—Climate Friend or Foe? Science News. Available online: https://www.sciencenewsdigital.org/sciencenews/june_8__2019/MobilePagedArticle.action?articleId=1491783#articleId1491783 (accessed on 15 December 2020).
9. Brewer, P.G.; Peltzer, E.T.; Walz, P.; Aya, I.; Yamane, K.; Kojima, R.; Nakajima, Y.; Nakayama, N.; Haugan, P.; Johannessen, T. Deep ocean experiments with fossil fuel $CO_2$: Creation and sensing of a controlled plume at 4 km depth. *J. Mar. Res.* **2005**, *63*, 9–33. [CrossRef]
10. Davis, A.R.; Oliver, B.G. A vibrational-spectroscopic study of the species present in the $CO_2$-$H_2O$ system. *J. Solut. Chem.* **1972**, *1*, 329–339. [CrossRef]
11. Dickson, A.G. Introduction to CO2 Chemistry in Sea Water. Available online: https://www.iaea.org/sites/default/files/18/07/oa-dickson-chemistry-1901015.pdf (accessed on 8 January 2020).
12. Dunk, R.M.; Peltzer, E.T.; Walz, P.M.; Brewer, P.G. Seeing a deep ocean $CO_2$ enrichment experiment in a new light: Laser Raman detection of dissolved $CO_2$ in seawater. *Environ. Sci. Technol.* **2005**, *39*, 9630–9636. [CrossRef] [PubMed]
13. Zhang, X.; Kirkwood, W.J.; Walz, P.M.; Peltzer, E.T.; Brewer, P.G. A review of advances in deep-ocean Raman spectroscopy. *Appl. Spectrosc.* **2012**, *66*, 237–249. [CrossRef] [PubMed]
14. Yang, D.; Guo, J.; Liu, Q.; Luo, Z.; Yan, J.; Zheng, R. Highly sensitive Raman system for dissolved gas analysis in water. *Appl. Opt.* **2016**, *55*, 7744–7748. [CrossRef] [PubMed]
15. Brouillette, C.; Chetan Shende, C.; Farquharson, D.S.; Farquharson, S. A simple multi-pass optical system for Raman spectral measurements of ppm bicarbonate and carbonate in water. *J. Raman Spectrosc.* **2020**, submitted.
16. Farquharson, S.; Brouillette, C.; Shende, C.; Morrison, C. Measurement of $CO_2$ in water from a UV oxidizer by Raman Spectroscopy". *Adv. Space Res.* **2021**, in preparation.
17. Brewer, P.R. Ocean chemistry of the fossil fuel $CO_2$ signal: The haline signal of "business as usual". *Geophys. Res. Lett.* **1997**, *24*, 1367–1369. [CrossRef]
18. Omand, M.M.; Govindarajan, R.; He, J.; Mahadevan, A. Sinking flux of particulate organic matter in the oceans: Sensitivity to particle characteristics. *Sci. Rep.* **2020**, *10*, 5582–5598. [CrossRef] [PubMed]
19. Cross, P.C.; Burnham, J.; Leighton, P.A. The Raman Spectrum and the Structure of Water. *JACS* **1937**, *59*, 1134–1147. [CrossRef]
20. Falcke, H.; Eberle, S.H. Raman Spectroscopic Identification of Carbonic Acid. *Water Res.* **1990**, *24*, 685. [CrossRef]
21. Fung, K.H.; Tang, I.N. Relative Raman Scattering Cross-Section Measurements with Suspended Particles. *Appl. Spectrosc.* **1991**, *45*, 734–737. [CrossRef]
22. Thor Labs Product Literature, at UV Fused Quartz Cuvettes. Available online: thorlabs.com (accessed on 15 December 2020).
23. Savitzky, A.; Golay, M.J.E. Smoothing and differentiation of data by simplified least squares procedures. *Anal. Chem.* **1964**, *36*, 1627–1639. [CrossRef]
24. Raman, C.V. The Molecular Scattering of Light: The Colour of the Sea, Nobel Lecture December 11, 1930, Stockholm, Sweden. Available online: https://www.nobelprize.org/nobel_prizes/physics/laureates/1930/raman-lecture.pdf (accessed on 15 December 2020).